A helium atom scattering study of the growth of platinum on nickel (100)



2005 J. Phys.: Condens. Matter 17 7455

(http://iopscience.iop.org/0953-8984/17/48/001)

INSTITUTE OF PHYSICS PUBLISHING JOURNAL OF PHYSICS: CONDENSED MATTER

J. Phys.: Condens. Matter **17** (2005) 7455–7463 doi:10.1088/0953-8984/17/48/001

# A helium atom scattering study of the growth of platinum on nickel (100)

**D A MacLaren and W Allison**

Cavendish Laboratory, University of Cambridge, Madingley Road, Cambridge CB3 0HE, UK

E-mail: dam30@cam.ac.uk

Received 26 July 2005
Published 11 November 2005
Online at stacks.iop.org/JPhysCM/17/7455

**Abstract**

The growth of thin platinum films on a nickel (100) substrate is investigated by helium atom scattering. Growth is shown to be disordered for all temperatures between 150 and 600 K, resulting in continual surface roughening and an absence of atomically flat terraces. We separate growth into three main regimes. First, at temperatures below 250 K, growth is three-dimensional and is described using a 'hit and stick' regime of limited adatom mobility. Between 250 and 370 K, deposited films remain three-dimensionally rough but involve intermixing of Pt and Ni. At temperatures above 370 K, large three-dimensional structures are absent and alloying is extensive, occurring via a sequence of thermally activated and well-defined alloy phases. Complete alloying occurs above 650 K.

(Some figures in this article are in colour only in the electronic version)

## 1. Introduction

Nickel and platinum catalysts are used extensively in industrial applications, particularly for processing hydrocarbon feedstocks [1], and their alloys are interesting because they promise *tunable* catalytic activity and selectivity [1–3]. An appealing fabrication process for such alloys is the thin-film growth of platinum onto a nickel substrate, which would minimize the mass of expensive platinum required and may provide a route to surface structures that cannot be achieved from a bulk alloy precursor. It is critical, however, to understand the thermal stability of such systems, as most industrially viable catalysts must be capable of operation at elevated temperatures without degradation. In this paper, we will address both the surface structure and the thermal stability of one such thin-film platinum system: the growth of platinum on a nickel (100) substrate (hereafter referred to as 'Pt/Ni(100)').

We begin with a brief consideration of bulk nickel–platinum (NiPt) alloys, as they represent the thermodynamic minimum to which surface alloys, created by thin-film deposition, will tend. NiPt alloys are one of the most studied alloy systems [4, 5] but until recently were difficult

  

to model accurately, largely because their structures arise from a delicate balance of entropic, surface tension and elastic terms in the system's free energy [4–8]. For example, surface-energy considerations alone predict surface segregation of Ni [9–11]; in practice, only (110)-terminated crystals demonstrate such an effect, with both (100) and (111) crystals favouring surface Pt enrichment. In spite of a large (11.6%) lattice mismatch, a slight exothermic enthalpy of formation [12, 13] gives rise to random substitutional (fcc) alloys across the whole alloy system and ordered alloys for the specific stoichiometric ratios of $Ni_3Pt$ and NiPt. The alloys are also observed to have oscillatory compositions in their uppermost 3–5 atomic layers [4]. Laterally, reconstructions are observed for (100) surfaces: a shifted row reconstruction for surface platinum concentrations between 13% and 65% and a pseudo-hexagonal phase above 65% [14].

With such complex behaviour in the equilibrated alloy, it is to be expected that the thin-film growth of Pt/Ni(100) will also exhibit a rich and temperature-dependent phenomenology. Segregation effects may favour stability of a platinum overlayer, predicting layer-by-layer growth. On the other hand, the large lattice mismatch and greater electron affinity of Pt compared to Ni could force an island growth mechanism. In contrast to Pt growth on Ni(111), where experiments indicated an initial layer-by-layer growth mechanism, very little research has been conducted on the growth of Pt/Ni(100). Deckers *et al* [12] and Egawa *et al* [2] suggested that two-dimensional, layerwise growth occurs up to 8 ML, citing as evidence possible break-points in Auger electron and x-ray photoemission spectroscopy curves respectively. By monolayer coverage, however, Deckers noted the absence of a LEED pattern, indicating significant surface disorder that is difficult to reconcile with true epitaxial growth. Weak $(1 \times 1)$ LEED spots only recurred following an anneal to 520 K, whilst annealing to 620 K produced a relaxed surface alloy. Amongst the variety of surface analytical tools available [15], we have previously demonstrated [16] helium atom scattering (HAS) to be suited to studies of thin-film growth, especially when surface order and disorder is of interest [17, 18]. We therefore apply HAS here to determine unambiguously the growth mode for the first few monolayers, and also to observe the subsequent alloying behaviour.

## 2. Experimental details

All experiments were conducted using the Cambridge helium atom diffractometer, which is described in detail elsewhere [19]. Thin-film growth and alloying was observed with a beam energy of 70 meV, which was calibrated by measuring the interference fringes arising from atoms scattered from adjacent, exposed lattice planes on a lightly sputtered Ni(100) surface. Platinum deposition was performed with a custom-built electron-beam evaporator. Before use, the Ni(100) was cleaned by repeated argon ion bombardment (800 eV, 30 min, 300 K, $\sim 7\ \mu$A cm$^{-2}$) and annealing (773 K, 30 min; 1000 K, 30 s), until the helium specular reflectivity was reproducibly intense. The chamber base pressure was below $5 \times 10^{-10}$ mbar, with residual gas measured to comprise predominantly of $H_2$ and CO, both of which are known to adsorb onto the reactive Ni(100) surface below surface temperatures of $\sim$400 K [20, 21] and could potentially alter the observed growth mode. For example, atomic hydrogen has been observed to affect Ni adatom mobility [22], whilst several studies of Pt homoepitaxy have demonstrated a strong variation in growth mode with low concentrations of CO [23, 24]. We therefore measured the adsorption rate directly by observing the decay in specular reflectivity with time [17], obtaining an adsorption rate below 5% ML per hour at 120 K, the lowest temperature used in this study. Such low contamination rates are not problematic over a typical experimental timescale, but where appropriate, contamination was minimized by holding the crystal at 450 K until needed, then cooling quickly to take data.

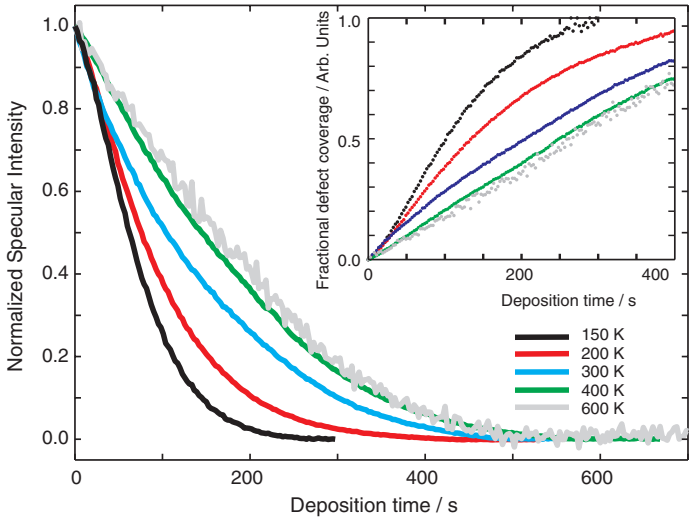


**Figure 1.** The growth of platinum on Ni(100) at various substrate temperatures observed under in-phase scattering conditions (for Ni—36.5° incidence, 70 meV). Inset: variation of defect coverage for the initial stages of platinum deposition; see text for details.

## 3. Results and discussion

### *3.1. Deposition*

Our key results are presented in figure 1, which plots the variation of helium specular reflectivity during the deposition of platinum onto Ni(100) at various substrate temperatures. Data are normalized by first subtracting the background signal and then dividing by the initial intensity, correcting automatically for thermal attenuation. Note that this normalization procedure results in the data for the highest substrate temperature appearing noisier, as Debye–Waller effects [17] attenuate the absolute signal.

The data of figure 1 are particularly easy to interpret. No oscillations are observed in the deposition curves at any substrate temperature and each curve decreases monotonically, even for longer deposition times than those illustrated. HAS growth oscillations are an excellent indication of layerwise growth [17] and their absence here demonstrates unambiguously that the initial growth of Pt/Ni(100) does not proceed by a simple layer-by-layer mechanism. As confirmation of surface disorder, diffraction scans taken after several different deposition times and temperatures did not reveal any HAS diffraction features, unlike the clean Ni(100) surface [20]. Furthermore, there is no evidence within the temperature range studied of the 're-entrant growth' observed in Pt homoepitaxy [23]. A lack of growth oscillations or break points in the data makes coverage calibration difficult; however, if we interpret the data as implying three-dimensional growth, then we may compare the reduction in reflectivity observed here with that observed in other three-dimensional Pt growth systems [23] to conclude that the deposition in figure 1 is consistent with platinum coverages of two to three monolayers. Clearly, this calibration is subject to variations in the scattering cross-section of Pt that arise from differences in our scattering conditions; however, it is sufficient for the approximation required here and the deposition rate is consistent with the expected performance of the apparatus used.

Each curve of figure 1 is recorded at an 'in-phase' scattering condition (for Ni(100)) and so is sensitive primarily to the total diffuse scattering and is a good measure of the surface defect

density during processing. Assuming that the specular amplitude is directly proportional to the defect-free surface area, then the measured specular intensity will be given by the square of the scattered amplitude [17]. Thus, the fractional total defect cross-section, $\chi$, is given by

$$\chi = 1 - \sqrt{\frac{I}{I_0}}, \tag{1}$$

where $I_0$ is the specular intensity for reflection from the clean surface. For example, in systems of isolated adsorbates, $\chi$ is given by the product of adsorbate density and the scattering cross-section per adsorbate, whereas in stepped systems, $\chi$ is the product of step scattering cross-section per unit length and the total step length. Here, we plot the variation of $\chi$ during Pt growth in the inset to figure 1. Note that these data indicate a difference between growth above and below 400 K. Above 400 K, surface defect coverage increases linearly with Pt deposition across the data set; below 400 K, a linear variation is lost before a fractional coverage of 0.7. Linearity in the data indicates a growth mechanism with little overlap of scattering cross-sections and is consistent with continuous step roughening, three-dimensional roughening or an increase in isolated defect structures. Loss of linearity, on the other hand, implies that scattering centres become sufficiently numerous that their cross-sections begin to overlap. We conclude from figure 1, therefore, that roughening increases with Pt deposition at all substrate temperatures, but with the roughest surfaces grown at low temperatures, where adatom mobility is lowest.

It is not possible to assign the observed surface roughness to specific structural details using figure 1 alone, although a structural dependence on temperature is apparent. The decrease in diffuse scattering between 140 and 400 K may result from a greater surface adatom mobility and hence the formation of larger surface islands. Much less change is observed between 400 and 600 K, indicative of a similar morphology throughout this temperature range. Even at 600 K, however, where adatoms might be expected to overcome most diffusional kinetic barriers, platinum adsorption still roughens the surface. Three-dimensional growth is often caused by a high kinetic barrier to inter-terrace diffusion (the 'Ehrlich–Schwoebel barrier'), but at substrate temperatures of 600 K, we calculate this to imply a barrier of $\sim$1.5 eV, which is unlikely. As we will show, surface alloying provides a more appropriate explanation.

To understand the thin-film structures better, figure 2 shows two 'lattice-rod scans' of the Ni(100) surface after deposition of a thin platinum layer. The curves plot the variation in surface reflectivity with perpendicular momentum transfer, taken here with a fixed beam energy and by varying the angle of incidence. Neither curve exhibits the interference oscillations that are characteristic of atomically-flat step or island structures [17], much as predicted from our discussion of figure 1. Nevertheless, there are significant, reproducible differences between the two lattice-rod scans. The 500 K curve is comparable to that observed on the clean Ni(100) surface, albeit with lower intensity. Together with the occasional observation of very weak HAS diffraction features (not illustrated here) and the previous observation [12] that a (1 $\times$ 1) LEED pattern could be observed, the high-temperature lattice-rod scan implies a predominantly two-dimensional, but atomically corrugated surface structure. In the context of the additional evidence outlined below, we interpret the data as implying the incorporation of Pt into the Ni lattice and the formation of a surface alloy. In contrast, the lattice-rod scan of the thin film deposited at 150 K curve is significantly attenuated, particularly at low $k_z$. The attenuation is consistent with an atomically rough surface whilst the 'shadowing' at low $k_z$ can be attributed to taller, three-dimensional structures on the surface attenuating the helium beam at near-grazing incidence. A similar effect was observed from structures formed during the growth of cobalt on copper (111) [25].

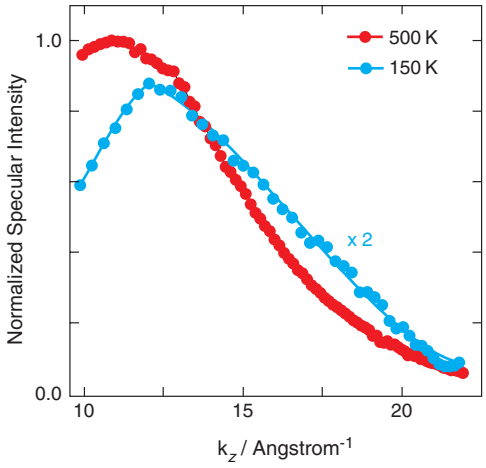


**Figure 2.** Lattice-rod scans of low-coverage platinum films grown at 150 and 500 K. Specular intensity is plotted versus the perpendicular momentum transfer. Platinum deposition was halted after 50% and 75% reductions in the specular reflectivity for the 500 and 150 K data sets respectively.

### *3.2. Alloying*

To explore the possibility of alloying further, the evolution of thin films was monitored during annealing. The results of one such set of scans are presented in figure 3, which concentrates on the behaviour above room temperature, where effects due to CO adsorption are minimized. Here, Pt was deposited at room temperature until saturation of the reflectivity—we estimate a coverage of 2–3 monolayers. The three data sets each plot surface reflectivity versus temperature as the Pt/Ni(100) is first heated, and then cooled, at a constant rate. For clarity, three annealing cycles are illustrated separately, although in practice they were conducted in immediate sequence; the surface was first heated from 300 to 550 K, then cooled to 300 K (data set (a)) before heating and cooling to maximum temperatures of 650 K (data set (b)) and 780 K (data set (c)). Note that the particular details of the annealing cycles are not critical and all the main features discussed below were evident when the thin film was heated uniformly from room temperature to 780 K. Each data set is plotted on a logarithmic intensity axis, such that the simple exponential trend expected of Debye–Waller attenuation [17] appears linear. Any deviations from a linear trend indicate changes in surface reflectivity and hence changes in surface structure.

Starting with figure 3(a), there are two substantial deviations from the exponential trend. Surface reflectivity falls initially with temperature, before rising sharply between 370 and 400 K. Specular reflectivity then drops slightly, before a second, broader increase in reflectivity begins at ∼435 K. This second rise continues until 530 K, increasing reflectivity by a further 40%. Thereafter, the crystal was cooled back to room temperature. A shallow exponential increase in reflectivity upon cooling leads to only 45% increase in reflectivity over the starting point, despite the larger changes observed during heating. Fitting an exponential Debye–Waller trend to the data taken during cooling yields a fitted surface Debye temperature of 812 K (taking the substrate mass as that of nickel). Such a large value is unrealistic, being far larger than the bulk values for either nickel (375 K) or platinum (230 K), and instead indicates that the surface structure continues to change during cooling and that the surface becomes rougher once more.

Figure 3(b) plots Pt/Ni(100) reflectivity immediately after the processing of figure 3(a) and as the crystal is heated to 650 K, then cooled. In contrast to figure 3(a), the strong feature

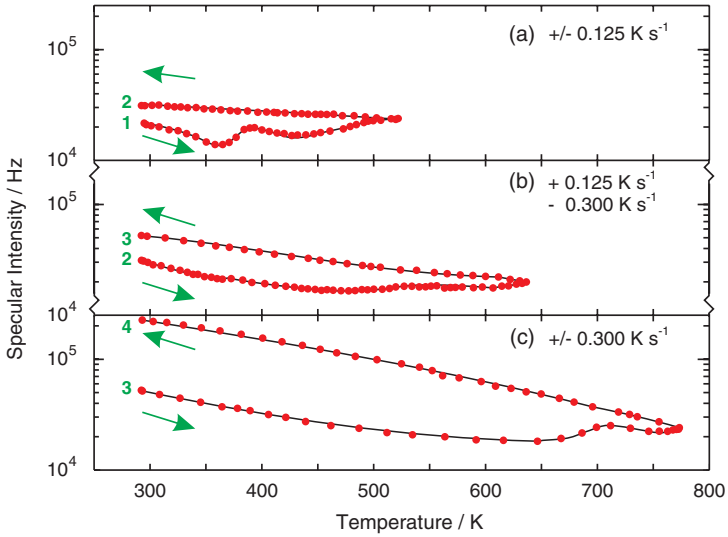


**Figure 3.** Thermal processing of a Pt/Ni(100) system grown at room temperature. Arrows indicate the annealing cycles (points 1 to 2, 2 to 3 and 3 to 4 respectively) and the heating/cooling rates are as indicated. Data sets (a)–(c) were taken in immediate succession and are only separated for clarity. Intensity axes are logarithmic, implying that the expected attenuation due to Debye–Waller scattering appears linear: all deviations from the linear trend indicate changes to surface morphology.

at 435 K is now absent and thermal attenuation dominates until a surface temperature of 485 K, when surface smoothing again occurs. At 650 K, the crystal is cooled back to room temperature, producing a 68% increase in reflectivity with respect to the start of this second cycle.

Finally, figure 3(c) records the Pt/Ni(100) reflectivity subsequent to the above processing and as the crystal temperature is cycled from room temperature to 780 K and back again. Debye–Waller attenuation now dominates to a surface temperature of 650 K; none of the previous peaks are evident. A rise in reflectivity is observed between 650 and 715 K. Heating was continued to 780 K, after which the crystal is cooled back to room temperature. The final reflectivity is over four times higher than that of the start of figure 3(c) and has increased by an order of magnitude with respect to the reflectivity immediately after Pt deposition.

The data presented in figure 3 indicate several transitions between room temperature and 750 K. The transitions are irreversible and only appear the first time a temperature is reached. Presumably the system is moving from one metastable state to another. On the other hand, the structures formed at the maximum temperature of each cycle are not necessarily 'frozen-in' upon cooling, an effect most pronounced in the cooling portion of figure 3(a). The implications of these observations will be discussed in more detail below.

### *3.3. Discussion*

Our results demonstrate that platinum growth on Ni(100) is disordered at all temperatures between 150 and 600 K and does not result in the formation of structures that are ordered sufficiently to scatter helium coherently. Unlike earlier measurements [2, 12], growth under the conditions of the present experiment is best described by a disordered mechanism that produces three-dimensional structures at low temperatures. Both deposition curves and lattice-

rod scans of the Pt/Ni(100) surface suggested that growth at low temperatures differs from that above 400 K, a claim confirmed by changes in surface morphology observed during annealing at 400 K and illustrated in figure 3. Thermal processing produces further structural changes across a broad temperature range, from room temperature up to 750 K, each resulting in a less defective and more reflective surface.

We reconcile the above data by describing the growth of Pt/Ni(100) in terms of alloy formation, which is in accordance with its exothermic nature [12, 13], the high miscibility of Pt in Ni [26] and the known alloying at elevated temperatures [12, 13]. On the basis of our results and previous field ionization microscopy (FIM) observations [27], growth of Pt/Ni(100) can be separated into three main temperature regimes: below 250 K; between 250 and 370 K; and above 370 K. Below a deposition temperature of 250 K, FIM measurements demonstrate that surface alloy formation is unlikely and the present results show that diffusion of Pt adatoms is kinetically limited. Thus, a 'hit and stick' regime operates, where adatoms have insufficient energy to migrate across the substrate surface and so remain at the point of adsorption. Equilibrium structures, such as islands, cannot form and growth is rough and defective. Our assignment of three-dimensionally rough, non-epitaxial growth also better describes the loss of $(1 \times 1)$ LEED spots observed elsewhere [12] and is still compatible with previous Auger and x-ray spectroscopic studies [2, 12], where the lack of strong breakpoints make a clear assignment of growth difficult.

Although no change is observed in the HAS data, FIM data [27] imply that submonolayer deposition of platinum on Ni(100) results in surface alloy formation at all temperatures above 250 K. Platinum exchanges with the top nickel layer to form a random surface alloy. The HAS data presented here demonstrate a reduction of reflectivity but a lack of lattice-rod oscillations upon Pt deposition, indicating an increased density of defects which are unable to coalesce to form regions that scatter helium coherently. Thus, initial alloy formation either results in significant roughening and reconstruction of Ni(100), or hinders the mobility of displaced nickel adatoms, perhaps by pinning them to alloyed Pt sites. The former process is feasible as compositional changes are known to cause lattice relaxations in all NiPt alloys [4], driven either by the increased lattice strain due to incorporation of Pt, or by Pt's known driving force towards a close-packed Pt overlayer. If this process does occur, then it must do so on a localized scale and in an aperiodic manner, since no HAS diffractive features were observed.

Growth of Pt beyond the monolayer stage should differ from sub-monolayer growth, as the previous analysis suggests that super-monolayer growth will occur on top of a disordered alloy layer. Evidently, platinum adsorption on this rough surface continues to cause surface roughening, as neither clear breaks in the deposition curves (figure 1) nor changes in lattice-rod scans are observed, irrespective of surface temperature. Defects and surface roughness propagate through the growing platinum film, causing an initially linear increase in surface roughness with deposition, which is similar to recent predictions for the roughening of nickel growth on copper [28] but is significantly different to the homoepitaxy of Pt(111), which occurs via a two-dimensional, layer-by-layer mechanism below 340 K [23]. As noted in section 2, platinum homoepitaxy is influenced by the presence of molecular CO [24], which could also influence the growth of Pt/Ni(100) but is unlikely in the present study, given the CO concentrations outlined previously.

Thermal treatment of Pt/Ni(100) (figure 3) highlights at least three distinct alloying phases, starting at 370, 435 and 650 K. It is not possible to determine the precise nature of each phase change from the data presented here, although with reference to the literature the most likely changes can be suggested. The lowest change, at 370 K, is irreversible, causes only a modest increase in specular reflectivity and is likely to reflect an increased mobility of surface platinum adatoms, perhaps by initiating inter-terrace smoothing by allowing adatom diffusion across

rough step edges. The smoothing of three-dimensional surface structures is consistent with the differences between lattice-rod scans taken at 150 and 500 K respectively, but must still result in an aperiodic and corrugated surface.

The second thermal feature, between 435 and 530 K, is consistent with the onset of alloying, indicated previously by LEED to have occurred by a substrate temperature of 520 K [12]. What is interesting is that this change may be slightly reversible, which manifested here as an unrealistic fitted surface Debye temperature to the cooling curve of figure 3(a). Although less well-developed, a similar feature is observed during the second heating cycle. This phase of alloying was also observed (not shown here) to be less well-developed for low platinum coverages, in agreement with the model of platinum adsorption occurring via growth of an alloyed layer followed by rough, three-dimensional platinum growth. The peak at 435 K would then correspond to the onset of crystallinity and alloying in the upper platinum layers. The product of this transition remains disordered—or at least corrugated in an aperiodic manner—as the alloy reflectivity is still far below the terminal value in figure 3(c). Finally, the largest increase in surface reflectivity observed in this study started at a substrate temperature of 650 K, which corresponds well with the onset of full alloying observed previously in LEED.

As final comments, we note that there is good agreement between the HAS data of Pt/Ni(100) presented here and previous low-energy ion scattering (LEIS) measurements [14, 29] of the bulk alloys $Pt_{10}Ni_{90}(100)$ and $Pt_{25}Ni_{75}(100)$. The discrete transitions observed here between 400 and 650 K correspond well with the LEIS observation of a general 10% increase in surface platinum concentrations between 300 and 600 K. The largest HAS peak, starting at 650 K, is at a significantly lower temperature than that at which bulk equilibration is observed in LEIS (between 750 and 1000 K), but is consistent with the onset of alloying observed in the Pt/Ni(100) system by Deckers [12]. The lower transition temperature of the present work may be because the retreat of Pt from the surface is facilitated by the highly defective nature of the platinum film. A further interesting observation is that LEIS also observed compositional variations during cooling, consistent with the trend revealed in figure 3(a), with HAS. Thus, surface composition does not depend solely on kinetic barriers being overcome, such as that to bulk diffusion, but also upon the intricate thermodynamic considerations which give rise to a temperature-dependent segregation effect.

## 4. Conclusion

Helium atom scattering has demonstrated unambiguously that the growth of platinum on Ni(100) does not occur by a true layer-by-layer growth mechanism, but proceeds by the formation of defective, rough films. With reference to the literature, we have described the dominant growth mechanisms. At low temperature, low platinum mobility prevents the formation of coherently scattering domains and results in the formation of rough, three-dimensional islands. Above a substrate temperature of 250 K, adsorbed platinum alloys with the Ni(100) surface, again resulting in a rough film upon which defective, three-dimensional islands form. Above 400 K, surface smoothing can occur, although aperiodic, atomic-scale corrugations remain. Several stages of alloying are evident, most notably at 370 and 485 K. Complete alloying occurs at a substrate temperature of 650 K.

## References

[1] Rodriguez J A 1996 *Surf. Sci. Rep.* **24** 126
[2] Egawa C, Endo S, Iwai H and Oki S 2001 *Surf. Sci.* **474** 14
[3] Gauthier Y, Baudoing R, Joly Y, Rundgren J, Bertolini J C and Massardier J 1985 *Surf. Sci.* **162** 342

[4] Bardi U 1994 *Rep. Prog. Phys.* **57** 939
[5] Polak M and Rubinovich L 2000 *Surf. Sci. Rep.* **38** 127
[6] Légaré P, Cabeza G F and Castellani N J 1999 *Surf. Sci.* **441** 461
[7] Tréglia G and Legrand B 1987 *Phys. Rev.* B **35** 4338
[8] Legrand B and Tréglia G 1990 *Phys. Rev.* B **41** 4422
[9] Williams F L and Nason D 1974 *Surf. Sci.* **45** 377
[10] Bertolini J C, Massardier J, Delichere P, Tardy B and Imelik B 1982 *Surf. Sci.* **119** 95
[11] Deckers S, Habraken F H P, van der Weg W F, Denier van der Gon A W, Pluis B and van der Veen J F 1990 *Phys. Rev.* B **42** 3253
[12] Deckers S, Bisschop F, de Jager D, Offerhaus S H, van Roijen J, Habraken F H P M and van der Weg W F 1991 *Surf. Sci.* **258** 82
[13] Deckers S, Offerhaus S, Habraken F H P M and van der Weg W F 1990 *Surf. Sci.* **237** 203
[14] Hebenstreit W, Ritz G, Biedermann A and Varga P 1997 *Surf. Sci.* **388** 150
[15] Woodruff D P and Delchar T A 1994 *Modern Techniques of Surface Science* 2nd edn (Cambridge: Cambridge University Press)
[16] MacLaren D A, Bacon R T, Allison W, O'Connor D J, Dastoor P C, Noakes T C Q and Bailey P 2004 *Phys. Rev.* B **70** 125403
[17] Poelsema B and Comsa G 1989 *Scattering of Thermal Energy Atoms* (*Springer Tracts in Modern Physics* vol 115) (Berlin: Springer)
[18] Farías D and Rieder K 1998 *Rep. Prog. Phys.* **61** 1575
[19] Graham A, McCash E and Allison W 1995 *Phys. Rev.* B **51** 5306
[20] Rieder K H and Wilsch H 1983 *Surf. Sci.* **131** 245
[21] Johnson S and Madix R J 1981 *Surf. Sci.* **108** 77
[22] Huag K, Zhang Z, John D, Walters C F, Zehner D M and Plummer W E 1997 *Phys. Rev.* B **55** R10233
[23] Kunkel R, Poelsema B, Verheij L K and Comsa G 1990 *Phys. Rev. Lett.* **65** 733
[24] Kalff M, Comsa G and Michely T 1998 *Phys. Rev. Lett.* **81** 1255
[25] Dastoor P C 1994 *PhD Thesis* University of Cambridge
[26] Smithells C J 1992 *Smithells Metals Reference Book* 7th edn (London: Butterworth-Heinemann)
[27] Kellogg G L 1992 *Surf. Sci.* **266** 18
[28] Yang Y G, Johnson R A and Wadley H N G 2002 *Surf. Sci.* **499** 141
[29] Schmid M, Biedermann A, Böhmig S D, Weigand P and Varga P 1994 *Surf. Sci.* **318** 289